

Quantitative 3D microstructural analysis of naturally deformed amphibolite from the Southern Alps (Italy): microstructures, CPO and seismic anisotropy from a fossil extensional margin

MICHELE ZUCALI^{1*}, VALENTINA BARBERINI², MARCO VOLTOLINI³,
BACHIR OULADDIAF⁴, DANIEL CHATEIGNER⁵, LUCIA MANCINI⁶ &
LUCA LUTTEROTTI⁵

¹*DST – Dipartimento di Scienze della Terra ‘A. Desio’, Università degli Studi di Milano,
Via Mangiagalli 34–20133 Milan, Italy*

²*Dipartimento di Scienze dell’Ambiente e del Territorio e di Scienze della Terra,
Università degli Studi di Milano-Bicocca, Piazza della Scienza 4, 20126 Milan, Italy*

³*Earth Science Division, Lawrence Berkeley National Laboratory, #1 Cyclotron Rd.,
Berkeley, CA 94720, USA*

⁴*Institut Laue-Langevin, 38042 Grenoble Cedex 9 France, 6, Rue Jules Horowitz, B.P.156*

⁵*CRISMAT-ENSICAEN and IUT-Caen, Université de Caen Basse-Normandie,
campus 26, Bd. M. Juin 14050 Caen, France*

⁶*Elettra – Sincrotrone Trieste S.C.p.A., S.S. 14, km 163,5 in Area Science Park,
34149 Basovizza, Trieste, Italy*

**Corresponding author (e-mail: Michele.Zucali@unimi.it)*

Abstract: The anisotropy of a rock is intimately related to the development of shape-preferred orientations (SPOs) and crystallographic-preferred orientations (CPOs). Quantifying the three-dimensional (3D) CPOs and SPOs in natural rocks is therefore critical for understanding the processes underlying the development of anisotropy. In this work, we present a CPO study of six amphibolite samples from the western Southern Alps (Italy) that have been characterized previously. Quantitative texture analyses using neutron diffraction data provided 3D CPOs for amphibole and plagioclase and were used to calculate seismic properties. We describe the relations between mesoscopic foliation and lineation, crystallographic fabrics and seismic anisotropies for lower–middle crust amphibolites. Based on these relations and in the context of lower–middle crust within fossil extensional margin, we suggest that seismic profiles should display large-scale geological features commonly present in extensional tectonics, such as folds and shear zones, rather than flat-lying structures. Moreover, from the integration of CPOs with geological data, we observe that samples from the Strona Ceneri boundary are characterized by a granulite to amphibolite facies transition while those from the Scisti dei Laghi only record the amphibolite facies evolution, supporting the idea of two independent tectono-metamorphic units pre-dating the amphibolite re-equilibration.

During large-scale geodynamic processes, the lithosphere responds to tectonic movement and related directional stresses. This response may vary from mega- to microscopic scales and produces unique structures and anisotropy at all scales. Anisotropy is commonly produced by the rearrangement of the shapes of grains (shape-preferred orientation or SPO) and the crystallographic-preferred orientation (CPO) based on the pressure and temperature conditions during deformation (Babuska and Cara

1991; Tommasi *et al.* 2001; Ji and Xia 2002; Karato 2008; Liang *et al.* 2008). Quantifying the three-dimensional (3D) CPOs in natural rocks is crucial to understanding the processes underlying the development of anisotropy. Observed seismic anisotropy is controlled by the properties of rocks and is often used to make inferences on the large-scale behaviour of the Earth’s crust and mantle. In the last two decades, several studies have shown the first-order influence of CPO on seismic

properties and the importance of describing quantitatively the CPO of rock-forming minerals in crustal and mantle rocks (e.g. Mainprice *et al.* 1993; Rabbel and Mooney 1996; Tatham *et al.* 2008; Lloyd *et al.* 2011b).

Quantitative CPO studies are typically performed using electron backscatter diffraction (EBSD) and U-stage, commonly devoted to the study of grain-scale processes with a very local approach in two dimensions, or using a statistical approach by X-ray and neutron diffraction, in the latter cases studying larger volumes (up to 1 cm³). In the first approach, EBSD is the most advanced and widely used technique. It is capable of linking CPO and SPO at the granular scale and it is spatially resolved, but 3D reconstruction of the microstructure can be lengthy and is often not practical. The second approach, which is less commonly used for geological samples, is devoted to quantitative texture analyses of rocks and other anisotropic materials.

In this study, we present CPO data obtained by neutron diffraction. This approach allows us to investigate relatively large volumes of rocks (c. 1 cm³), comparable in size to those investigated by experimental seismic velocity measurements (Kern *et al.* 1996, 2009; Kitamura 2006).

In particular, we applied this approach to six amphibolite samples from the continental crust (Serie dei Laghi and Ivrea Verbano units) of the Southern Alps that have been studied by Barberini *et al.* (2007). Although the seismic velocities of all samples were measured using the pulse transmission technique (Birch 1960, 1961), two samples were studied using the U-stage technique to obtain the CPO.

To quantify the CPO for all of the samples in 3D and compare the results with measured seismic velocities, we used CPO analyses from neutron diffraction data, applying the maximum Entropy-Williams-Imhof-Matthies-Vinel approach (EWIMV; Matthies and Vinel 1982; Sakata *et al.* 1993) to solve the orientation distribution function (ODF) from CPO measured on large (c. 1 cm³) samples at the high-flux neutron source of the Institut Laue Langevin (ILL; Grenoble, France).

The CPO data are constrained by microstructural analysis using a petrographic microscope. Macroscopically, our amphibolite rocks have millimetre-thick foliation defined by mineral layering (amphibole and plagioclase-rich layers) and the preferred orientation of amphibole. Amphibole-rich layers are characterized by foliated/lineated-to-massive fabrics with relicts of garnet and pyroxene, whereas plagioclase is organized in elongated aggregates.

The CPO analysis results are used to calculate seismic properties, which have also been computed with a thermodynamic approach, using bulk

chemical compositions (Connolly and Kerrick 2002; Connolly 2005). The CPOs, seismic properties calculated using CPO measurements, bulk chemical composition and experimental laboratory measurements (Barberini *et al.* 2007) are discussed in terms of geodynamic processes in an extensional regime recorded in fossil continental crust (Serie dei Laghi and Ivrea Verbano zone, Southern Alps).

Geological setting and sample description

The samples were collected in the western Southern Alps (Italy; see Barberini *et al.* 2007, fig. 1). The Southern Alps are interpreted as a portion of the Permo-Triassic passive margin with the African plate (Muttoni *et al.* 2003). The basement rocks record pre-Mesozoic metamorphic and magmatic imprints (Peressini *et al.* 2007) followed by a Permo-Mesozoic high-temperature imprint, which is likely related to extensional geodynamics leading to the opening of the Tethys Ocean (Spalla and Marotta 2007).

The samples were collected in the Southern Alpine domain of the Western Alps (Fig. 1), in the Serie dei Laghi and Ivrea Verbano units (Boriani *et al.* 1990c). The Serie dei Laghi consists of two units: an upper unit (Strona Ceneri) composed of meta-siliciclastic sediments and a lower unit (Scisti dei Laghi) that mainly consists of medium-grade schists. In the Strona Ceneri Border Zone, which defines the boundary between the two units, banded amphibolites are associated with paragneisses, quartz schist and garnet-staurolite-bearing mica-schist. Minor lenses of garnet-bearing amphibolite or retrogressed eclogite, metagabbro, pyroxenite and spinel peridotite are also present. Pressure and temperature estimates from amphibolites suggest that they experienced amphibolite facies metamorphism at $T \approx 600$ °C and $P \approx 6$ –8 kbar (Giobbi Mancini *et al.* 2003). Northwest of the Serie dei Laghi is the Ivrea Verbano zone which is dominated by a thick unit of variably migmatized metapelitic schists, known locally as the Kinzigite Formation which forms a layer that varies in thickness from few hundred metres to c. 3–4 km trending SW–NE. In the north-western part of the Ivrea Verbano zone, high-grade metapelites are inter-layered with bands of 1–200-m-thick amphibolite and ultramafic rocks. The southern part of the Ivrea Verbano zone is dominated by an intrusive layered mafic complex ('Mafic Formation' e.g. Rivalenti *et al.* 1981; Zingg 1983; Quick *et al.* 1994) that is c. 10 km wide and extends along-strike (NE) for nearly 40 km. The estimated conditions of the Permian metamorphic stage are P of 4.5–8 kbar and T of 650–850 °C (Henk *et al.* 1997; Vavra *et al.* 1999).

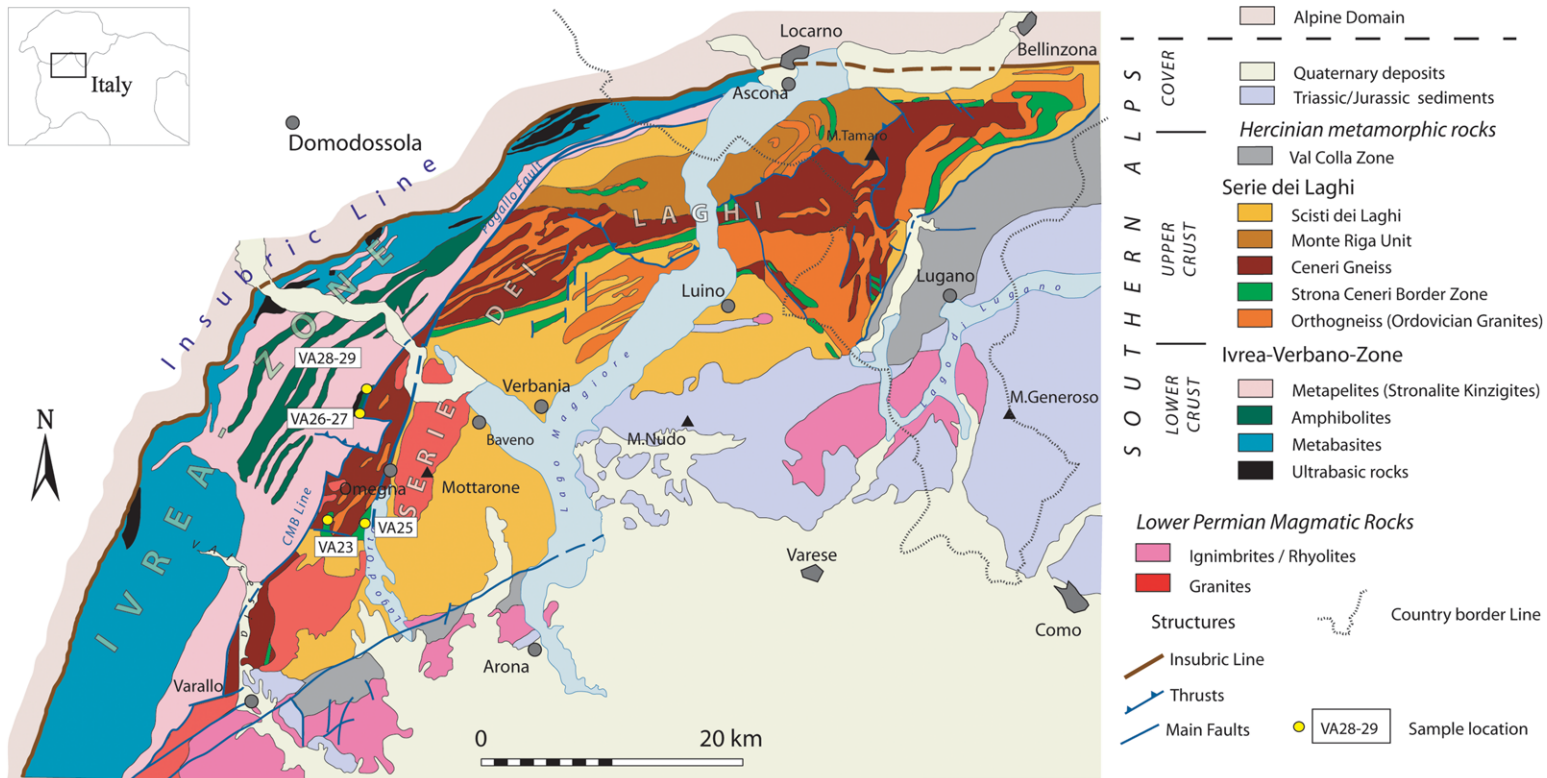
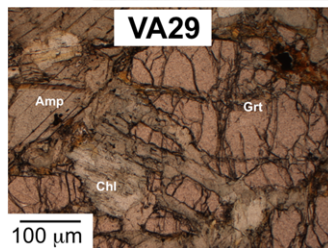
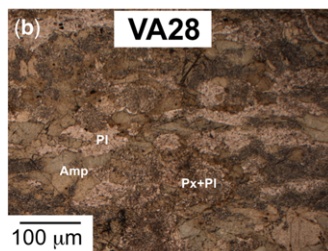
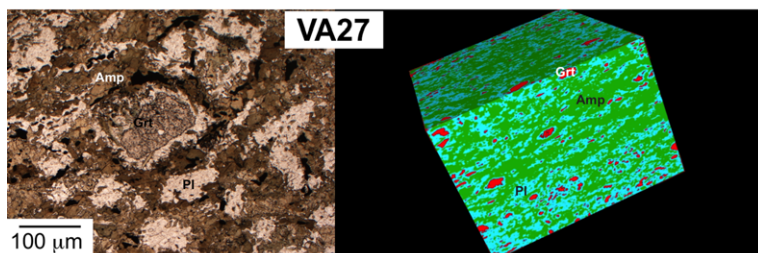
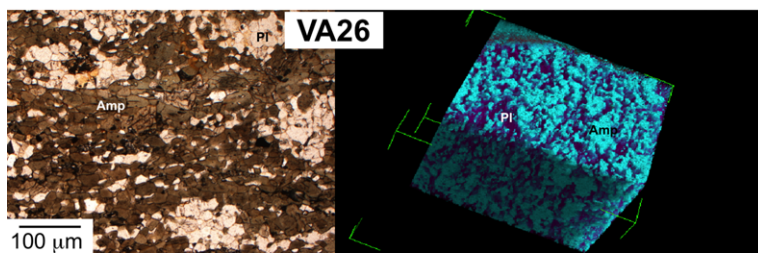
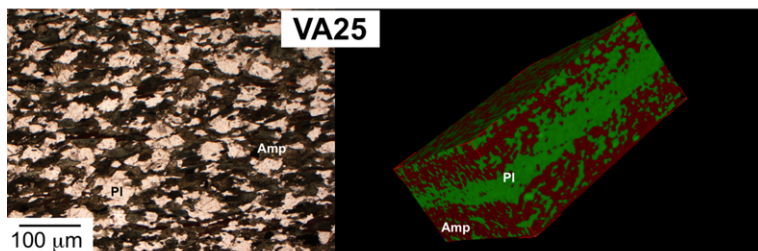
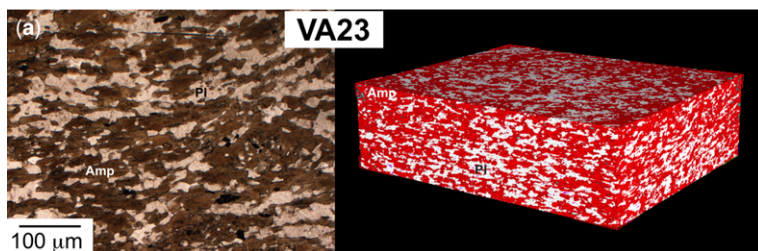


Fig. 1. Geologic map of the western Southern Alps (redrawn after Barberini *et al.* 2007). Sample location is also shown.



MODAL COMPOSITION (XRPD)						
	VA23	VA25	VA26	VA27	VA28	VA29
AMP	57	53	48	45	66	70
PL	21	38	44	40	20	16
QTZ	1					
BT		5				
CHL	10					
GRT				3	2	8
CPX				5	3	1
OPQ	1	1	1	3	1	1
SPH			4	3		
ALT	10	3	3	1	8	4

Amp=amphibole; Pl=plagioclase; Chl=chlorite;
 Bt=biotite; Qtz=quartz; Grt=garnet; Cpx=clinopyroxene;
 Sph=titanite; Opq=opaque minerals; Alt=alteration
 minerals (indistinguishable).

Sample descriptions

The samples were collected in three distinct areas of the Southern Alps and are characterized by differences in mineralogy and fabric. The samples of the first group (VA23 and VA25, inner part of the Strona Ceneri zone, Fig. 1) are plagioclase + amphibole lineated-foliated (LF)-tectonites (tectonites description after Turner and Weiss 1963). The samples of the second group (VA26 and VA27) differ in terms of fabric and mineralogy because garnet occurs or is replaced by aggregates of plagioclase, which controls the fabric. The third group of samples (VA28 and VA29) is similar to the second but differs in terms of the fabric, which is much weaker. Samples VA26, VA27, VA28 and VA29 were collected near the boundary between Strona Ceneri and Ivrea Verbano (Fig. 1).

Cubes of $c. 1 \times 1 \times 1$ cm (the same cubes used for neutron texture analyses; see the following paragraph) were analysed using X-ray computed tomography (CT). CT analyses were carried out in two ways: using standard X-ray laboratory equipment at the Department of Earth and Environmental Sciences, University of Milano-Bicocca, Milan, Italy (see Castellanza *et al.* 2008 for further details) and using synchrotron X-ray micro-tomography (SR-CT) at the SYRMEP beamline of the Elettra-Sincrotrone Trieste laboratory in Basovizza (Trieste), Italy (for further details see Baker *et al.* 2012; Zucali *et al.* 2014).

For both types of analyses, the tomography slices were combined using image analysis software (Voltolini *et al.* 2011). After appropriate filtering and thresholding, 3D reconstructions of the samples were obtained (Fig. 2a, b). Good results were obtained for samples VA23, VA25, VA26 and VA27, whereas the images for samples VA28 and VA29 were not satisfactory; this is likely because within the sample volume analysed, the density contrast between the minerals and the crystal size are poorly suited to producing CT images of good quality (it was impossible to discriminate every mineral phase from the others).

In the following sections we describe in detail the microstructure of our samples as observed using the petrographic microscope and CT scans.

VA23 + VA25

These samples are characterized by their simple and typical amphibole + plagioclase association; they both contain a penetrative planar fabric marked by the SPO of amphibole (Fig. 2a) and plagioclase occurs either as bands or lenses, displaying only localized SPO. Well-defined mineral layering occurs only in VA25 (Fig. 2a); plagioclase is locally substituted by thin aggregates of white mica which does not display SPO. The 3D tomographic images describe the planar fabric in VA25, which is associated with a mineral lineation marked by the SPO of amphibole grains. A similar mineral lineation is also visible in VA23, where amphibole SPO controls the development of the foliation planes.

VA26 + VA27

These samples have weak preferred orientations in the form of foliations or lineations. In VA26, the planar fabric is defined by amphibole aggregates (Fig. 2a) and isolated plagioclase aggregates in flattened lenses. The longest axis is parallel to the mineral lineation, which is best defined by the SPO of polycrystalline amphibole aggregates or the localized SPO of amphibole grains. In VA27, garnet occurs in isolated grains or porphyroblasts or is wrapped by the dominant foliation, which is marked by the SPO of amphibole or elongate amphibole aggregates. Plagioclase may occur as a corona around garnet porphyroblasts or as rounded lenses (Fig. 2a). Garnet and plagioclase fabrics are particularly well represented in the false-colour tomographic image, where the light-blue coronas of plagioclase occur around red garnet grains (Fig. 2a). The described microstructural relations suggest that garnet occurs as a relict of an older mineral association, likely representing the granulite facies

Fig. 2. (a) Microstructures of the studied samples. Left column: optical microphotographs under plane-polarized light. Right column: 3D reconstructions obtained from 2D X-ray CT scans. VA23 and VA25 show Amp and Pl associated in a penetrative planar fabric defined by Amp SPO, which is also very well described by 3D CT reconstruction. VA26 and VA27 also show planar fabric marked by Amp SPO. Plagioclase crystals are arranged in flattened lenses with the longest axis parallel to the mineral lineation defined by amphibole-preferred orientation. In addition, within VA27 garnet occurs as isolated grains, porphyroblasts wrapped by the dominant foliation. Plagioclase may occur as corona around garnet porphyroblasts or as rounded lenses, as well outlined by 3D CT reconstruction. (b) Microstructures of the studied samples, optical microphotographs under plane-polarized light. VA28 and VA29 are mainly characterized by alternate massive amphibole-rich layers and plagioclase-rich lenses. Plagioclase is replaced by thin aggregates of epidote and albite, amphibole is partly preserved, and chlorite and green-amphibole substitute hornblende grains. These mineralogical variations justify the poorer-quality of the CT images for these samples, not reported here. The table shows modal composition (vol%) of samples, determined with Rietveld method on X-ray powder diffraction data (after Barberini *et al.* 2007).

metamorphic stage that pre-dates the amphibolite facies stage.

VA28 + VA29

These samples are mainly characterized by alternating massive amphibole-rich layers and plagioclase-rich lenses. The amphibole SPO also marks a mineral lineation (X axis) within the amphibole-rich layers, whereas few plagioclase grains display an aspect ratio >1 with the long axis parallel to the lineation. Garnet porphyroblasts also occur (VA29) or are partially to completely replaced by fine aggregates of epidote and plagioclase (Fig. 2b). Similarly to VA26 and VA27, the microstructural features allow us to reconstruct an older granulite facies stage, predating the amphibolite facies metamorphism characterized by amphibole + plagioclase mineral paragenesis.

Neutron diffraction texture analysis (CPO)

Quantitative texture analysis using neutron diffraction allows for the investigation of volumes of rock of the order 1 cm^3 in a relatively short time (few hours) due to the high-penetration power of neutrons in matter and the high flux available at the nuclear reactor at the ILL (Zucali *et al.* 2002, 2010, 2012; Tartarotti *et al.* 2011). The lattice planes of the rock-forming minerals analysed are investigated in sample space and represented as pole figures (Fig. 3). Pole figures represent the directional distributions of the lattice plane normal (hkl) relative to the sample coordinates (e.g. mesoscopic foliation and lineation). Pole figures use equal-area projections of the orientation sphere and display pole densities in multiples of a random distribution (mrd) (Wenk 2006). Quantitative CPO analysis is represented as pole figures (hereafter referred to as PF, where the mesoscopic tectonic fabrics are reported as X , Y and Z directions (Fig. 3). The X direction is parallel to the mesoscopic mineral lineation, while the XY plane is the foliation plane. The quality of the refinement and the ODF calculation is assessed by reliability values (R in Table 1). Quantitative analysis of diffraction data has been carried out using Maud software (Lutterotti *et al.* 1999), and data are represented using the BearTEX software package (Wenk *et al.* 1998).

We present the results from the D19 diffractometer at the ILL (Fig. 3), where monochromatic radiation is used with a Cu (111) monochromator with a wavelength λ of 1.46 \AA , a flux of $\approx 10^7\text{ n cm}^{-2}\text{ s}^{-1}$ (where n = neutrons) and a maximum beam size of $10 \times 10\text{ mm}^2$. The intensities are measured by rotating the sample around two axes (φ and χ) with a texture goniometer (Fig. 3) and

a step interval of 5° . A position-sensitive detector (<http://www.ill.eu/instruments-support/>) with an angular range of $120 \times 30^\circ$ is used to acquire simultaneously diffracting lattice planes at different Bragg angles.

In the PFs presented (Fig. 4), the foliation plane trace (XY plane) is the horizontal diameter. According to the crystal symmetry, the PFs may or may not represent the direct crystallographic axes; in the presented cases, only poles to the (010) planes of amphibole actually correspond to [010] axes. For all other PFs, the represented directions correspond to the direction normal to the labelled planes, that is $[hkl]^*$ reciprocal directions.

Below we describe in detail the CPO of our samples as obtained from neutron diffraction texture analyses.

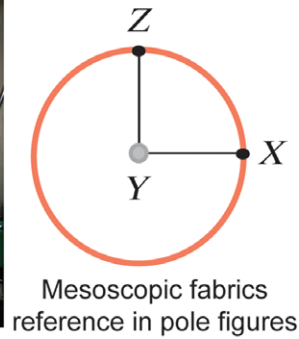
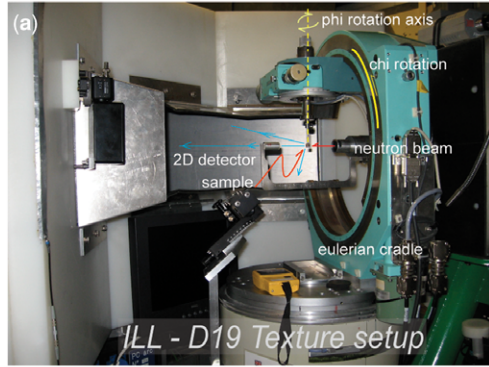
VA23 + VA25

In these samples, amphibole is characterized by similar distributions of the main crystallographic planes. In particular, the (100) poles describe a cluster distribution at an angle of $c. 35\text{--}45^\circ$ to the X lineation direction and to the XY foliation plane. Conversely, the (010) and (001) poles describe the girdle distributions, particularly (001), which describes a girdle containing Y , with a maximum at an angle of $<30^\circ$ to the Y axis.

Plagioclase CPOs are defined by weak (100) poles distributed along girdles at low angles to the foliation plane, whereas the (010) and (001) poles produce small circles with a rotation axis broadly distributed at 45° to the X axis within the XY plane.

VA26 + VA27

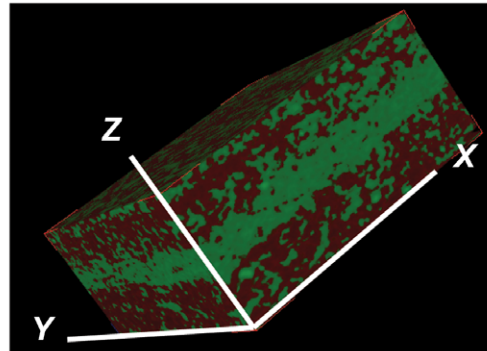
As these samples do not have well-defined macroscopic foliation, the mesoscopic fabric orientations are less reliable. The samples were placed under the neutron beam with reference to the weak SPO visible to the naked eye. With this limitation in mind, the (001) poles of amphibole in VA26 are clustered close ($<10^\circ$) to the X mineral lineation direction, whereas the (100) and (010) poles describe girdle distributions with weak secondary maxima that are parallel to the YZ plane and at an angle of 30° to the Z direction. In VA27, the amphibole (001) poles display a similar distribution as for VA26 but with a rotation of $c. 30^\circ$ with respect to Y . The (010) and (100) poles also have corresponding relations. Plagioclase does not have a strong preferred orientation and is regarded as having a random crystallographic orientation distribution in VA26, with a maximum value is 1.09 mrd where a random distribution would be one. In particular, VA26 has a ring-like distribution around Y , but this



(b)

3D Mesoscopic
fabric reference

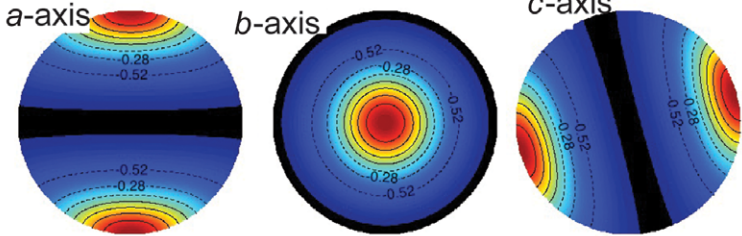
X - mineral lineation
XY - foliation plane
XZ - thin section plane



(c)

Standard lattice orientations
(no reference with mesoscopic fabrics)

Amphibole



Plagioclase

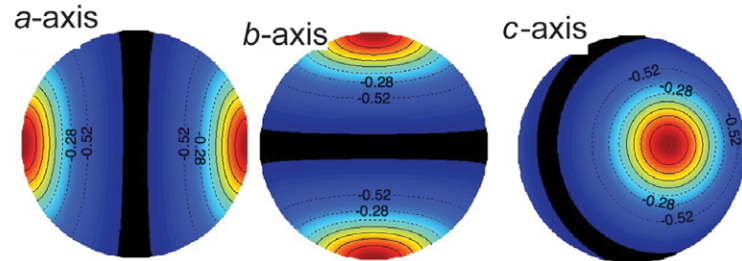


Fig. 3. (a) Geometry of the D19 beamline at Institut Laue-Langevin, Grenoble, France. (b) Mesoscopic fabric reference. (c) Standard lattice preferred orientation of amphibole and plagioclase single crystals.

Table 1. Refinement and ODF calculation reliability factors

Sample	Global factors			Mineral phase	Single phase factors		
	GoF	R_W	R_B		F^2	R_W	R_B
VA23	1.08	22.01	17.28	AMP	1.72	44	34
				PL	1.47	15	10
VA25	1.06	18.92	14.4	AMP	3.16	44	26
				PL	1.07	27	16
VA26	1.02	11.55	8.68	AMP	2.3	17	13
				PL	1.04	18	14
VA27	1.01	19.11	14.91	AMP	1.31	25.1	20.33
				PL	1.15	20.98	18.15
VA28	1.27	19.86	15.09	AMP	2.21	31	26
VA29	0.83	13.26	10.21	AMP	1.13	25.53	18.81
Mineral	Space group	a	b	c	alpha	beta	beta
Amphibole	C2/m	9.8	18.07	5.27	90		105.14
Albite	P-1	8.14	12.79	7.15	94.33	116.57	87.65

For each sample both global factors and factors for each mineral phase used within the calculations are listed. GoF: goodness of fit; R_W : intensity-weighted factor; F^2 : texture strength in mrd^2 ; R_B : R-Bragg factor.

distribution is related to noise during the data acquisition and processing.

In VA27, the (100) poles define clusters at $30-0^\circ$ to Z in the XZ plane and close to Y . The (001) poles plot from 45° to 0° to X in the XZ plane.

VA28 + VA29

In VA28, amphibole displays a well-defined (001) maximum in the X direction, whereas the (100) poles are dispersed along a girdle within the YZ plane with maxima at approximately 45° to Y . The (010) poles display composite girdle distributions, with one close to the XZ plane and one parallel to the YZ plane.

In VA29, amphibole is characterized by a less-pronounced CPO. In particular, the (010) poles are nearly randomly distributed whereas the (100) poles describe a cluster at 45° to X within the XZ plane and the (001) poles describe a girdle in a plane perpendicular to the XZ plane and at 45° to X , but perpendicular to the cluster of (100) poles. In both VA28 and VA29, the CPO of plagioclase is close to random as indicated by distribution densities below 1.10 mrd (Fig. 4). In VA29 however, the CPO of plagioclase is characterized by two small circles of (010) and (001) poles that are characterized by a rotation axis $c. 20^\circ$ to Z in the XZ plane. As previously described for VA26, nearly random distributions suffer from noise during data acquisition, which results in a preferred orientation that wrongly suggests a rotation around Y .

Among the studied samples, only the CPOs of VA28 and VA29 have been previously described (determined with the U-stage technique, Barberini

et al. 2007). According to Outlaw *et al.* (2000) and Barberini *et al.* (2007), [001] of amphibole lies parallel to X (VA28) or may define an angle, commonly $<20^\circ$ to X (VA29), whereas (100) defines a girdle around (001).

We obtained similar distributions for samples VA26 and VA28. For the other samples where only the new data are available, amphibole CPOs display similar orientations. Table 1 lists the reliability factors and texture strength factors for the samples and minerals investigated. The two methods produce different results for VA29, which is likely related to the large grain size of this sample and resulting statistics. Due to the large grain size, the number of grains measured by the U-stage is relatively low, resulting in a statistically unreliable preferred orientation. As shown by the reliability factors in Table 1, the number of crystallites measured by diffraction is also small, but higher and more reliable than measurements carried out using the U-stage. Low reliability factors in both techniques may have yielded significantly different CPOs in some cases. We have been able to measure plagioclase CPOs for all six samples with varied results.

VA23 and VA25 are characterized by similar CPOs, in agreement with the described CPOs for deformed plagioclase (e.g. Ji and Mainprice 1990; Shigematsu and Tanaka 1999; Passchier and Trouw 2005; Barreiro and Catalán 2012). VA26 and VA28 display a random distribution for all the crystallographic planes, whereas VA27 and VA29 are characterized by weak textures that differ from VA23 and VA25, suggesting different deformation mechanisms and active slip systems.

3D MICROSTRUCTURAL ANALYSIS OF SOUTHERN ALPS AMPHIBOLITE

Microstructural observations may be used to discuss such differences; VA23 and VA25 display plagioclase layers whereas in the other samples plagioclase crystals occur in rounded aggregates closely related to garnet porphyroblasts or microdomains. The static recrystallization of plagioclase

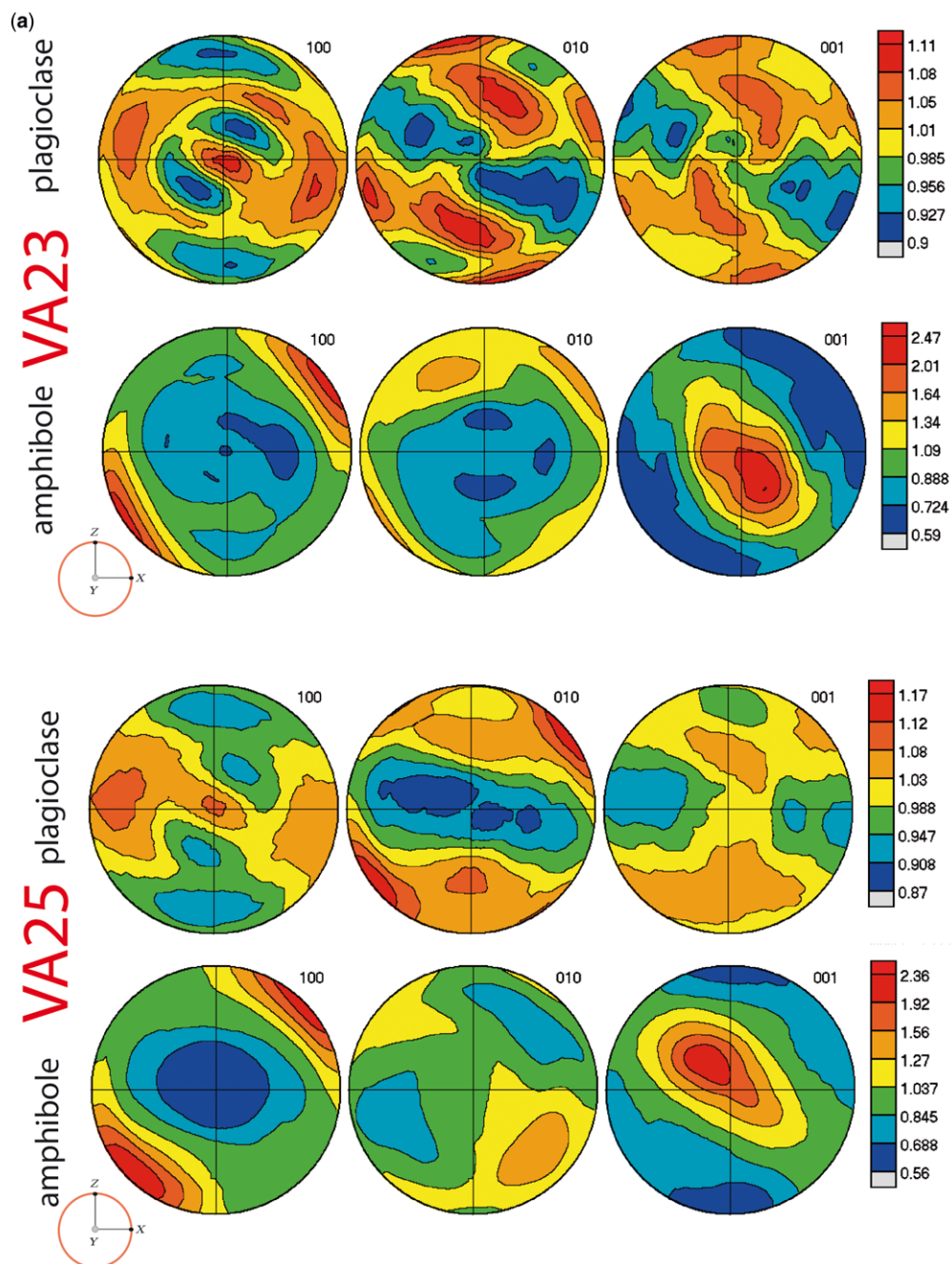
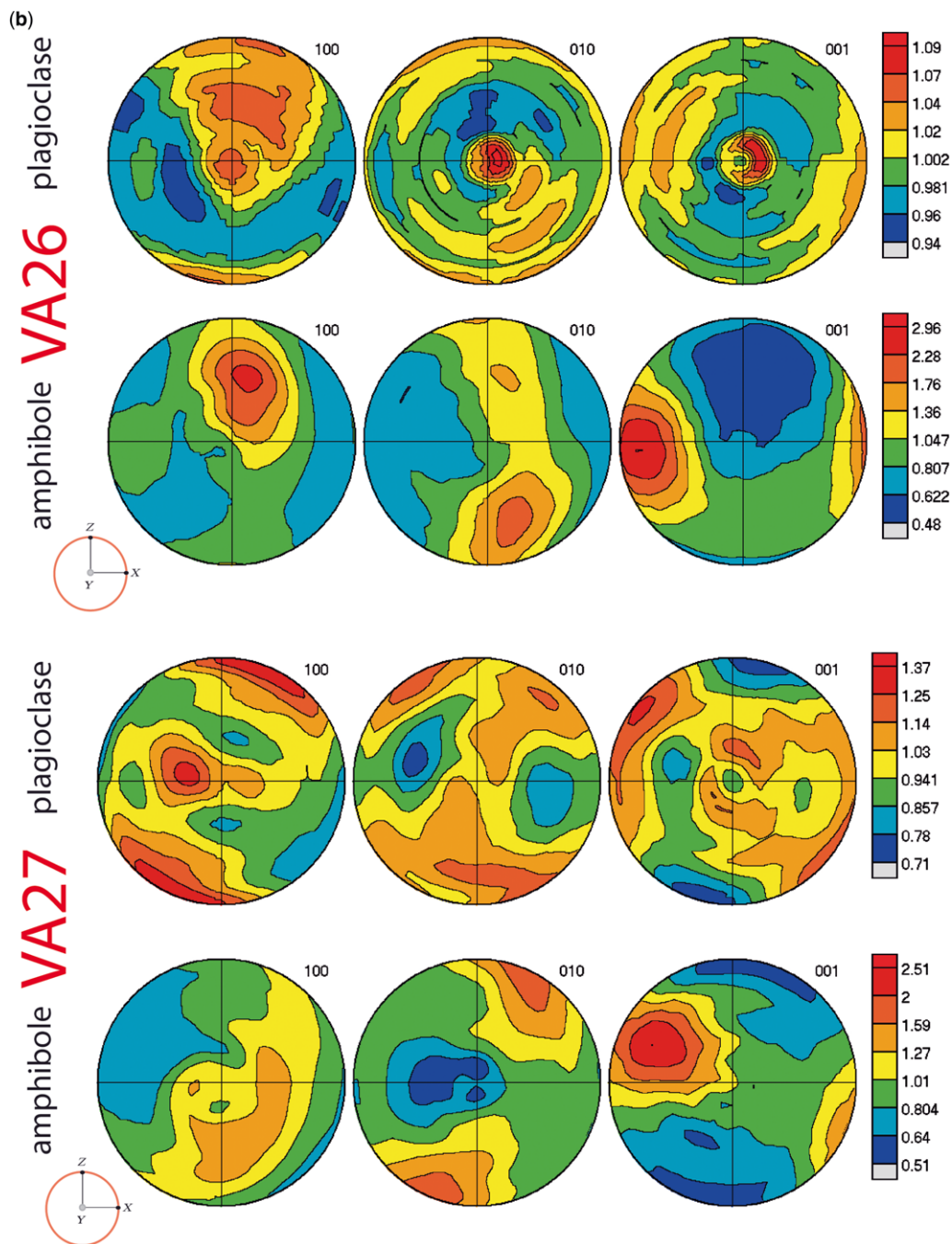


Fig. 4. Recalculated pole figures of the main crystallographic planes for amphibole and plagioclase, obtained from quantitative analysis of neutron diffraction data: (a) VA23 and VA25; (b) VA26 and VA27; and (c) VA28 and VA29.

Fig. 4. *Continued.*

in samples VA26, VA27, VA28 and VA29 may explain the absence of CPOs, whereas weak CPOs might have developed in domains where deformation occurred after plagioclase crystallization.

Seismic properties

In crustal rocks, seismic anisotropy may be caused by composition, mineralogy, CPO and SPO (Lloyd

3D MICROSTRUCTURAL ANALYSIS OF SOUTHERN ALPS AMPHIBOLITE

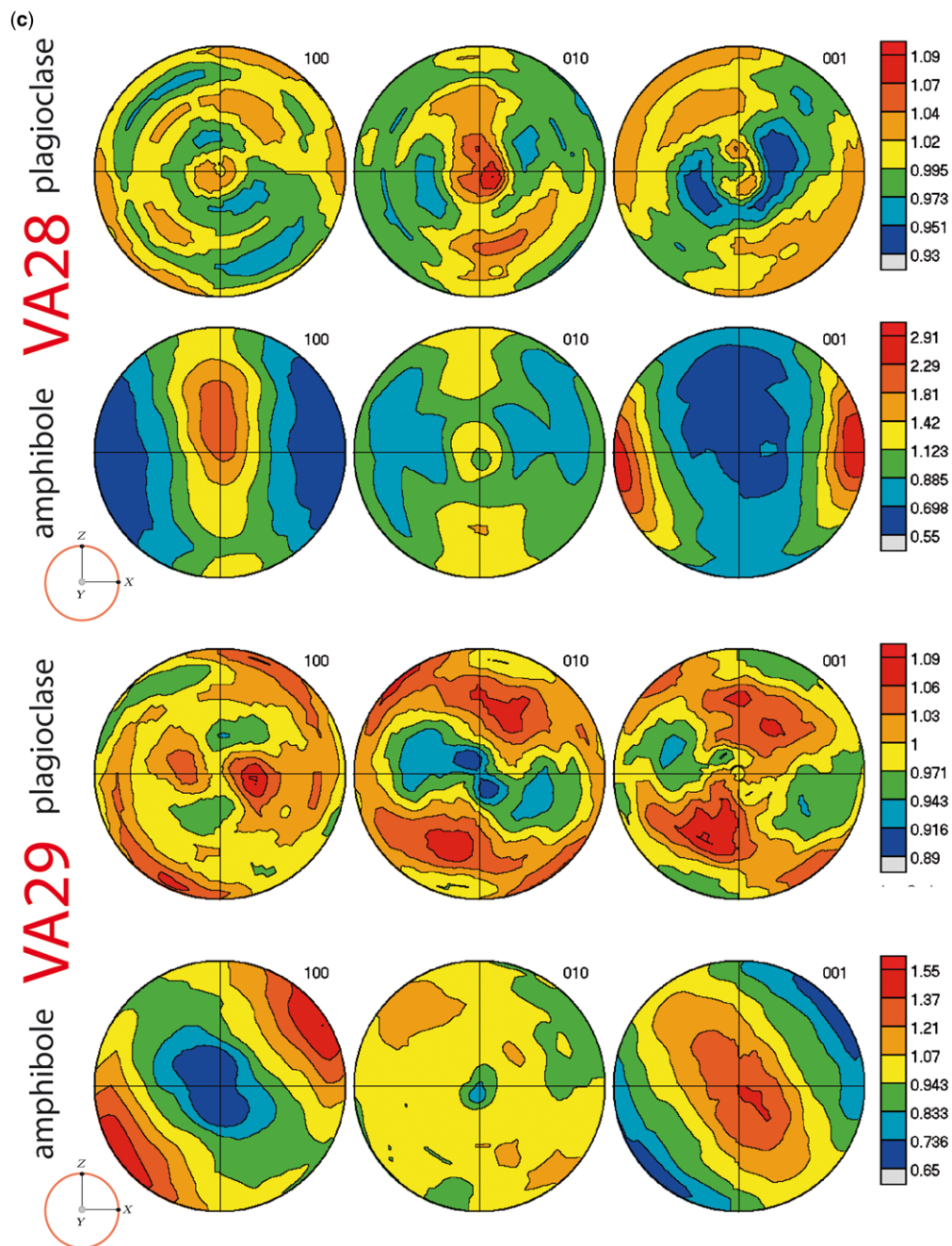


Fig. 4. Continued.

et al. 2011a). The petrofabric-derived seismic properties have been shown to match natural samples very well (e.g. Christensen 1984; Mainprice and Nicolas 1989; Siegesmund *et al.* 1989; Ji and Xia 2002).

In this section, we describe the seismic anisotropy of our samples as obtained using two different approaches. The first approach uses CPO data that are quantitatively expressed by the orientation distribution function (ODF) of rock-forming minerals

to average the single-crystal stiffness tensors. The theory, procedures and successful applications to natural rocks have been reported over the last two decades (e.g. Christensen 1984; Mainprice 1990; Lloyd *et al.* 2011a; Mainprice *et al.* 2011). In the second approach, seismic velocities are computed using the thermodynamic function G (molar Gibbs free energy). Within a given pressure and temperature interval and a rock system of interest, G is minimized to establish the stable mineral phases, their amounts and chemical compositions (see Connolly 2005 for details). The *Perple_X* software package (Connolly and Kerrick 2002; Connolly 2005) allows the stability fields and related seismic velocities to be calculated. The software requires the system (chemical) composition as molar units or weight fractions (percentage) as input.

This approach greatly differs from the approach that uses the crystallographic preferred orientations of rock-forming minerals (Mainprice 1990; Mainprice *et al.* 1993; Christensen and Mooney 1995; Ismaïl and Mainprice 1998). In the latter approach, the elastic properties of the polycrystal is averaged and weighted with the use of the distribution functions (ODF) for each mineral, whereas the thermodynamic approach assumes an isotropic material and does not consider the preferred orientation of minerals.

For stiffness tensors and densities, which are required in the first approach, we used those reported by Barberini *et al.* (2007). To average with respect to the ODF, we used the approach of Hill (1952). We used the *Beartex* software package (Wenk *et al.* 1998) to calculate the seismic velocities from the ODF, and the ODF input was calculated using the *Maud* software (Lutterotti *et al.* 1999) and neutron diffraction data.

As a reference, we calculated V_p for a simplified amphibolite consisting of a single crystal of amphibole and one of plagioclase (70% and 30% in volume, respectively). In this approximation, the elastic tensors used for the calculation are those of

the corresponding single crystals. Figure 5 displays the calculated V_p in km s^{-1} expected for single crystals of amphibole and plagioclase and for the modelled rock, which is obtained by averaging the contributions of single crystals of amphibole and plagioclase based on their relative volumes. The crystallographic axes are also shown for the V_p plots of amphibole and plagioclase, which allows the relations between lattice orientation and V_p anisotropy to be defined. Accordingly, the maximum V_p occurs parallel to the amphibole c -axis and plagioclase c - and b -axes, as has been shown in previous work (e.g. Siegesmund *et al.* 1989; Kitamura 2006; Barberini *et al.* 2007; Tatham *et al.* 2008).

In most samples, the highest V_p is in the plane of the foliation (XY) or at a relatively low angle to it (Fig. 6a, b). The orientation of the highest V_p is often close to the X direction (VA26, VA27, VA28), with some exceptions (VA23, VA25, VA29) where the maximum V_p are within the XY foliation plane but parallel to the Y direction. When the higher V_p describe a girdle (VA23, VA25, VA29), it is commonly at 45° between the XY and YZ planes. VA26 has a girdle at 45° between the XY and XZ planes. Conversely, in VA27 and VA28, the higher V_p describe clusters at 20° to X within the XZ plane (VA27) or parallel to X (VA28). The averaged V_p are in the range $6.2\text{--}7.0 \text{ km s}^{-1}$ and V_p anisotropy $1.97\text{--}3.18\%$.

Comparing the CPO pole figures with the V_p poles indicates that the directions normal to the (001) planes are the most important in the definition of the V_p anisotropy of amphiboles and of the rocks themselves. The plagioclase CPO is commonly very low and does not influence the overall V_p of the rock.

For the *Perple_X* calculations, the model system has been simplified to $\text{CaO-FeO-MgO-Al}_2\text{O}_3\text{-SiO}_2\text{-H}_2\text{O}$ (CFMASH) (Fig. 7). For solid solutions, we chose those of Dale *et al.* (2000) for amphibole, Newton *et al.* (1980) and Holland and Powell (1998) for garnet and that of White *et al.* (2001)

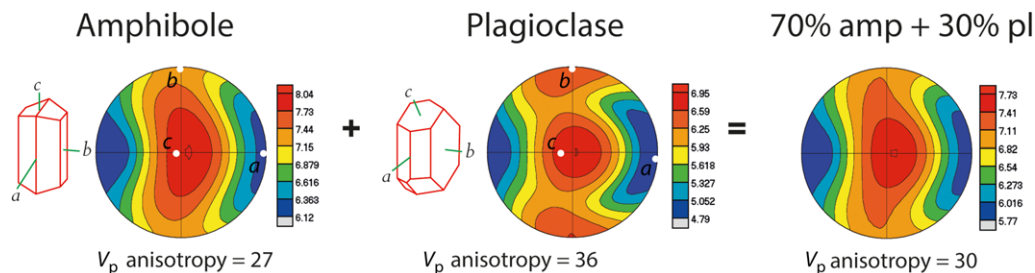


Fig. 5. 3D P-wave velocity (in km s^{-1}) for amphibole and plagioclase single crystals and for a hypothetical whole rock (amphibole 70% and plagioclase 30%). Crystallographic axes are shown for amphibole and plagioclase.

3D MICROSTRUCTURAL ANALYSIS OF SOUTHERN ALPS AMPHIBOLITE

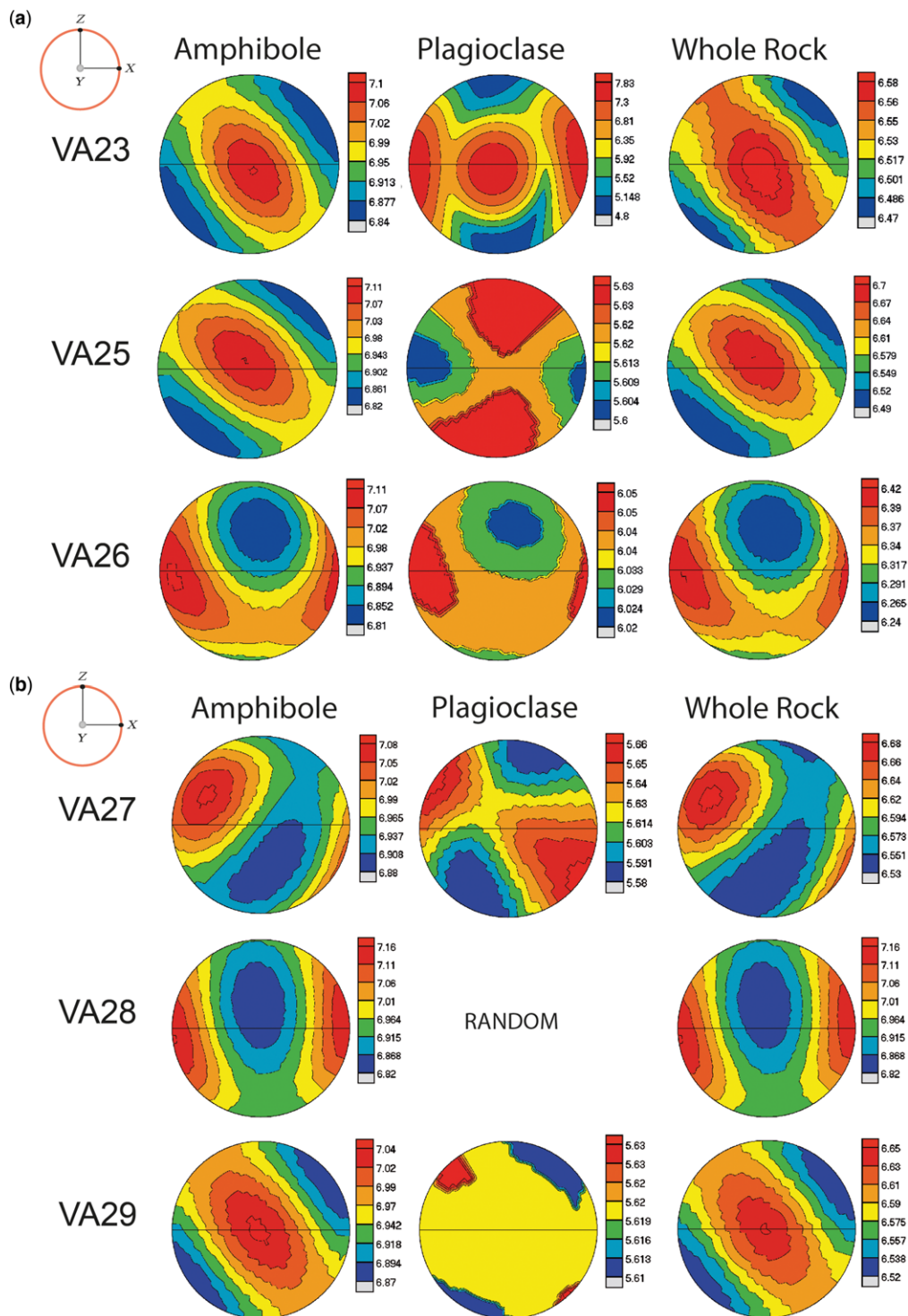


Fig. 6. (a, b) P-wave velocities distribution (in km s^{-1}) calculated from CPO data. V_p are presented separately for amphibole, plagioclase and averaged rock.

for granitic melt. Figure 7 presents the weight fractions (percentage) for each oxide used in the calculations and the V_p interval calculated in the pressure and temperature box, as inferred from the literature (see geological setting section).

Figure 8 and Table 2 synthesize the V_p values from the different methods used. In Figure 8, these data are also plotted with respect to the expected V_p range for a variety of amphibolite rocks from the middle–lower crust, as reported in the literature

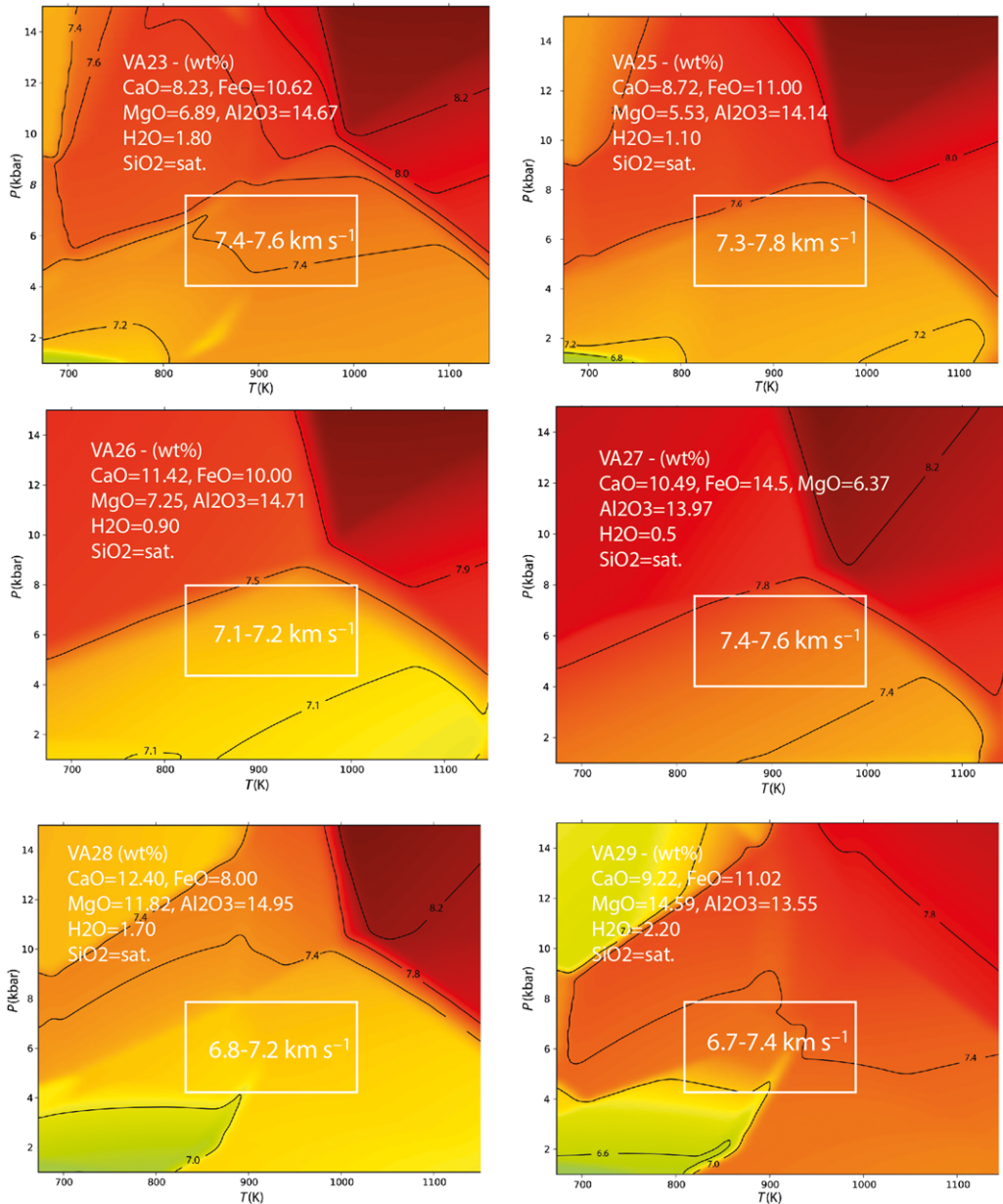


Fig. 7. V_p wave velocities distribution in the P – T field as calculated using *Perple_X* in the CFMASH model systems. Chemical compositions are calculated averaging chemical spot analyses with the modal amount of every mineral phase, in weight percentage (wt%); V_p intervals refers to the minimum and maximum values calculated by thermodynamic modelling; contour lines represents equal V_p lines.

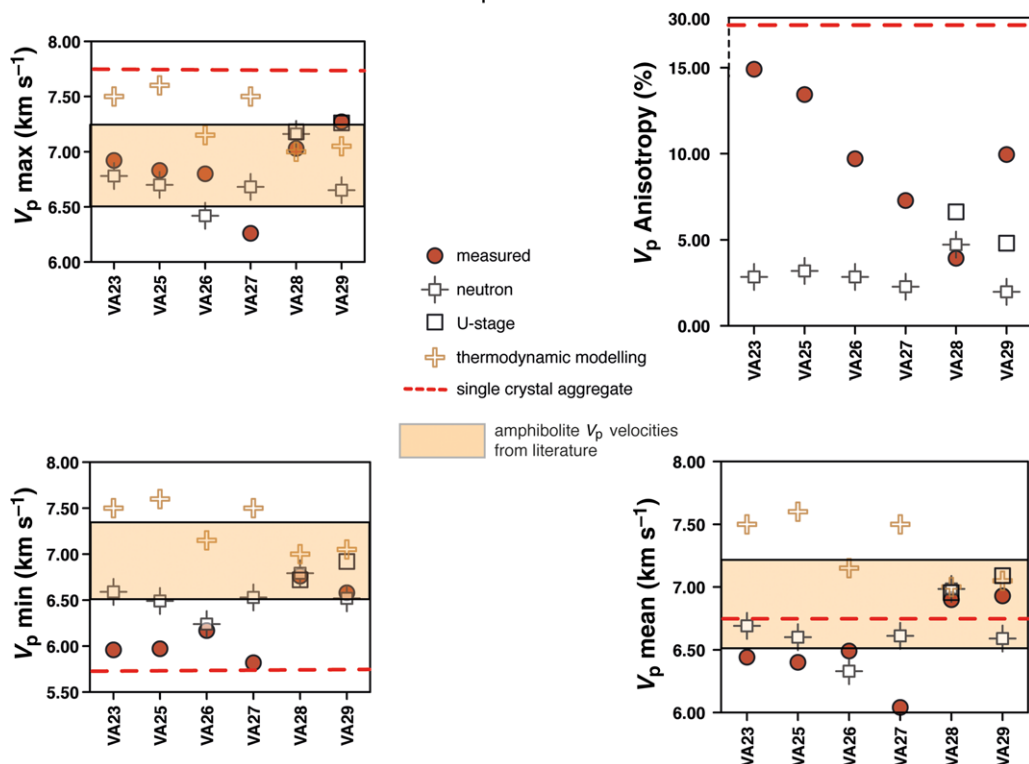
Amphibolite V_p wave velocities

Fig. 8. Graphical comparison of V_p data as obtained using various approaches described in the text. U-stage data and measured V_p are from Barberini *et al.* (2007) while literature velocities are from Siegesmund *et al.* (1989), Christensen & Mooney (1995), Kitamura (2006) and Tatham *et al.* (2008).

(Siegesmund *et al.* 1989; Christensen and Mooney 1995; Kitamura 2006; Tatham *et al.* 2008). This comparison highlights several aspects that deserve to be discussed in further detail.

The mean V_p calculated from the thermodynamic modelling are higher in VA23, VA25, VA26 and VA27, and they are similar for VA28 and VA29. No maximum or minimum values were calculated because the thermodynamic modelling does not consider any preferred orientations. In Figure 8, the values from the thermodynamic modelling are plotted with respect to the maximum and minimum V_p for reference. The U-stage-derived values agree for VA28 for all methods, but are higher in VA29. Similarly, the distribution of V_p derived from neutron data (Fig. 6b) in VA28 and VA29 resemble the distribution shown by Barberini *et al.* (2007). In particular, the higher-velocity girdle distribution in Figure 6b and in Barberini *et al.* (2007) differs by a rotation of 90° around Z. This rotation may be due to the poorly developed foliation/lineation in this sample. In general, the

measured and neutron-derived V_p values are in good agreement for most samples, with discrepancies of $<0.5 \text{ km s}^{-1}$. There is good agreement among all types of data for VA28, even for anisotropy which commonly displays larger differences between calculated and measured orientation data. VA26 also are in good agreement, particularly in the minimum and mean seismic velocities.

Discussion

Typically, the structures of passive margins are studied and described in terms of volumes of high or low velocities and densities based on information from deep seismic investigations coupled with gravimetric data (Contrucci *et al.* 2004). These studies have the largest impact on petroleum research along passive margins, particularly where extensional tectonics has created large basins that are now covered by salt deposits and are likely sites for large reservoirs (Lentini *et al.* 2010).

Table 2. Comparison of V_p wave velocities (km s^{-1}) data obtained from ultrasonic analysis, neutron diffraction analysis and U-stage CPO (Barberini et al. 2007).

	V_p measured				V_p calculated from LPO-neutron				V_p calculated from LPO-U-stage			
	x (km s^{-1})	z (km s^{-1})	Mean (km s^{-1})	Anisotropy (%)	Max (km s^{-1})	Min (km s^{-1})	Mean (km s^{-1})	Anisotropy (%)	Max (km s^{-1})	Min (km s^{-1})	Mean (km s^{-1})	Anisotropy (%)
VA23	6.92	5.96	6.44	14.91	6.58	6.47	6.53	1.69	n.a.	n.a.	n.a.	n.a.
VA25	6.83	5.97	6.40	13.44	6.70	6.49	6.60	3.18	n.a.	n.a.	n.a.	n.a.
VA26	6.80	6.17	6.49	9.71	6.42	6.24	6.33	2.84	n.a.	n.a.	n.a.	n.a.
VA27	6.26	5.82	6.04	7.28	6.68	6.53	6.61	2.27	n.a.	n.a.	n.a.	n.a.
VA28	7.03	6.76	6.90	3.92	7.16	6.82	6.99	4.86	7.18	6.72	6.95	6.62
VA29	7.27	6.58	6.93	9.96	6.65	6.52	6.59	1.97	7.26	6.92	7.09	4.80

3D MICROSTRUCTURAL ANALYSIS OF SOUTHERN ALPS AMPHIBOLITE

Most of the published seismic profiles display a transition between oceanic and continental crust through an ocean–continent transition, occasionally called an OCT, which is characterized by anomalous high-velocity/high-density layer(s) (Hirsch *et al.* 2009). The V_p of ‘normal’ continental crust varies between 5 and 8 km s⁻¹, generally increasing with depth, following a seismic stratigraphy typical of the continental crust (e.g. Christensen and Mooney 1995). Anomalous bodies in the ocean–continent transition zones may have a V_p above 6.7 km s⁻¹ (e.g. Blaich *et al.* 2011).

Studies of the lithostratigraphy and structural setting of fossil passive margins have shown that large- to small-scale folding that may be associated with the development of new fabrics is common (e.g. Bertotti *et al.* 1993; Spalla *et al.* 2000). Consequently, the distribution of lithotypes (i.e. bulk composition) is not linearly related to depth, such that mafic rocks (higher density) are more abundant in the lower crust whereas felsic rocks (lower density) are more common in the upper and intermediate crust (e.g. Christensen and Mooney 1995; Rudnick and Fountain 1995; Rudnick and Gao 2003).

The Southern Alps are commonly interpreted to be a portion of a Permo-Mesozoic passive margin of the African plate (Boriani *et al.* 1990*a, b, c*; Handy *et al.* 1999), and they are an ideal example for discussing the influence of rock anisotropy on the properties (e.g. seismic) of the rock (e.g. Rutter *et al.* 1999). The western sector of the Southern Alps is composed of continental crust rocks, from felsic to intermediate in composition, plus the Ivrea Body, a large mafic to ultramafic body (Bigi *et al.* 1990). This lithological association is commonly viewed as an outcropping section of the intermediate–lower crust transition (Boriani *et al.* 1990*b*; Rutter *et al.* 2007), tilted to between 20 and 60° during Triassic and Jurassic time and along the Insubric Line during the Alpine orogenesis (Boriani *et al.* 1990*b*; Barboza and Bergantz 2000).

The structural and petrological evolution and large-scale tectonics of this section have been studied as part of lithospheric-scale seismic investigations (Handy 1987; Boriani *et al.* 1990*c*; Rutter *et al.* 1999; Khazanehdari *et al.* 2000). The large heterogeneities in lithotype and the variety of scales (metres to kilometres) of folding and intrusive structures that characterize this fossil continental margin of the Southern Alps result in one of the most complex distributions of seismic wave velocities observed globally (Rutter *et al.* 1999; Lloyd *et al.* 2011*b*).

Modern studies of the distribution and behaviour of seismic velocities in crustal rocks have demonstrated how rock fabrics and folding may be exploited (e.g. using shear-wave splitting), which may vary due to foliation and CPO regardless of the

bulk composition (Rutter *et al.* 1999; Ji and Long 2006; Tatham *et al.* 2008; Lloyd *et al.* 2011*a*). As shown for passive margins globally and the Southern Alps in particular, foliations and CPO have been pervasively folded during and after syn-rifting tectonics (e.g. Alpine tectonics in the Southern Alps; Burlini and Fountain 1993).

The megascopic structural framework should be considered when defining the seismic model for interpretation. Burlini (1994) demonstrated seismic anisotropy recorded by 5–10-km-thick metapelitic layers, leading to shear-wave splitting times of up to 1.2 s. This anisotropy is strongly controlled by the CPOs and SPOs of sillimanite and biotite in high-grade melt-bearing metapelites (kinzigite) (Burlini 1994), associated with the amphibolites studied here.

We have confirmed that the seismic anisotropy is closely related to the CPO of amphibole in amphibolites (Siegesmund *et al.* 1989; Meissner *et al.* 2006; Tatham *et al.* 2008). In particular, the main mesoscopic and microscopic fabrics, which are generally characterized by alternating mineral layers, do not always correspond to the directions of the crystallographic anisotropy. This observation is due to the CPO of amphibole, which may be at an angle to the planar or linear fabrics that are well defined at the outcrop scale in hand samples and in seismic tomography. The SPO and CPO of plagioclase, which are the secondary rock-forming mineral in amphibolites, do not significantly affect the spatial distribution of anisotropy however; this remains controlled by the CPO of amphibole. This observation is in accordance with the ‘recipe’ approach by Azpiroz and Lloyd (2010); however, the SPO and CPO of plagioclase do contribute to lowering the average velocity (Tatham *et al.* 2008).

As shown by Lloyd *et al.* (2011*a, b*), shear-wave splitting and anisotropy may indicate changes in the orientations of rocks with depth. Because the shear-wave splitting of amphibolites is controlled by the CPO of amphibole, the reconstructed directions for these samples do not coincide with mesoscopic foliations or compositional layering; instead, they coincide with amphibole CPO fabrics. In our work the foliation plane (*XY*) and the CPO of amphibole may display orthorhombic symmetry (e.g. VA26 in Fig. 4*b* and VA28 in Fig. 4*c*), but they also differ by up to 20–30° (VA23 and VA25 in Fig. 4*a*, VA27 in Fig. 4*b* and VA29 in Fig. 4*c*), developing a monoclinic symmetry.

The deep 3D architecture of the western Southern Alps sector is characterized by large-scale folds that re-fold the rock boundaries, producing complex patterns of mutually folded layers and lenses of compositionally different rocks (Bigi *et al.* 1990). Within these crustal-scale lenses or layers the fabrics are equally complex, recording

multiple stages of superimposed deformation (Burlini 1994) which led to the development of various generations of foliations and lineations that cross-cut the main lithological boundaries. Several zones of strain localization are also recorded at different scales (Handy *et al.* 1999; Rutter *et al.* 2007), which developed under different metamorphic conditions and at different times during the tectono-metamorphic evolution of the area and were refolded locally during later stages (Khazanehdari *et al.* 2000). The ultramafic Ivrea Body occupies the south-westernmost part of the sector, adjacent to the Insubric Line, whereas kilometre-scale Permian granitic bodies localize in the eastern part of the sector (Fig. 1). The Ivrea Body is also internally characterized by well-developed fabrics and CPOs (Quick *et al.* 1995), whereas the intrusive granitic bodies are mainly isotropic. All these observations, together with metamorphic and magmatic age data of the western Southern Alps (Peressini *et al.* 2007; Luvizotto and Zack 2009; Mazzucchelli *et al.* 2010; Wolff *et al.* 2012), describe Ivrea Zone as constituted by rock units with contrasting tectono-metamorphic evolutions. This questions its interpretation as a vertical section through the lower crust, particularly in light of similar discussions on the settings of central portions of the Southern Alps (Spalla *et al.* 2005, 2010). In fact, Late Carboniferous–Early Permian granulite facies metamorphism and related deformation have been reported (Barboza and Bergantz 2000; Peressini *et al.* 2007) for the Ivrea Verbano rocks. Similarly, samples VA26, VA27, VA28 and VA29 collected near or within this unit are characterized by garnet relicts that pre-date the growth of the amphibolite facies paragenesis (plagioclase + amphibole). The CPOs of these samples also reflect this evolution; plagioclase is characterized by an absence or weakness of preferred orientations, whereas amphibole displays similar CPOs to the sample from the Scisti dei Laghi/Strona Ceneri (VA23, VA25). The absence of CPO in plagioclase is interpreted as linked to the origin of plagioclase, which replaces garnet during the decompression from granulite (eclogite?) to amphibolite conditions as confirmed by microstructural and tomographic image analysis (Fig. 2a, b) and thermobarometric estimates from the literature (Giobbi Mancini *et al.* 2003). Conversely, in VA23 and VA25 plagioclase CPO records the deformation associated with the amphibolite facies imprint, developing preferred orientation characteristic of plastic deformation at amphibolite facies conditions (see Passchier and Trouw 2005).

The combination of structural, metamorphic and petrochronological data, now constrained by CPO analysis, strongly suggest that we should interpret the evolution of western Southern Alps

crust as an active extensional margin since Late Carboniferous–Early Permian time that accommodated the opening of the Alpine Tethys (Stampfli and Borel 2002; Handy *et al.* 2010). The Ivrea Verbano granulite imprint was likely related to the onset of the asthenosphere uplift that culminated with the intrusion of the Mafic Body (Barboza and Bergantz 2000). The amphibolite facies imprint occurred as the Ivrea Verbano zone reached intermediate crustal levels and came into contact with the Scisti dei Laghi, through the Cossato-Mergozzo-Brissago shear zone (Boriani *et al.* 1990a; Boriani and Burlini 1995).

All these observations present us with a scenario that must be considered when interpreting the seismic data for a section of continental crust, although the general assumption is that extensional tectonics result in relatively simple large-scale structures. Firstly, the lithological/chemical variations in the crust are not necessarily simply related to depth, but they are uniquely controlled by the folding and deformational history of the pre-existing lithostratigraphy. Secondly, the macro- and microscopic fabrics have been repeatedly folded and locally replaced by new fabrics. Thirdly, the crystallographic fabrics may have orthorhombic to monoclinic symmetry with respect to the shape fabric (i.e. foliations and lineations), leading to more complicated relations between seismic anisotropy, crystallographic fabrics and mesoscopic (shape) fabrics.

Conclusions

To quantify the contribution of crystallographic fabric to the bulk seismic properties of rocks, we have analysed amphibolites from the western Southern Alps which are considered an example of fossil lower crust of the African side of the Tethys passive margin.

The results demonstrate that the contribution of CPO is of primary importance if we want to reconstruct fully the tectono-metamorphic evolution of the Southern Alps continental rocks. CPOs may give us clues about the past evolution of the area, which may be successfully used to show the contrasting geological history of adjacent areas.

Neutron diffraction CPO analysis results in a more reliable and accurate definition of the ODF for amphibole in 3D and enables the reconstruction of the plagioclase CPO, which was arbitrarily considered random by Barberini *et al.* (2007) for samples VA28 and VA29.

The combination of these new data with those published for pelitic rocks in the same area (Burlini and Fountain 1993), together with crustal-scale structures from this portion of the Southern Alps,

3D MICROSTRUCTURAL ANALYSIS OF SOUTHERN ALPS AMPHIBOLITE

emphasizes the importance of introducing structural data, such as crystallographic fabrics, into seismic models when reconstructing the structure of continental crust, as suggested by Lloyd *et al.* (2011a, b).

Future studies should integrate quantitative data from shape fabrics, for example from phase-contrast synchrotron X-ray microtomography (e.g. Baker *et al.* 2012; Zucali *et al.* 2014), into the computation of seismic properties, which will likely produce a more refined model relating the mesoscopic fabrics, microscopic preferred orientations and lattice anisotropies to the large-scale seismic response. Hopefully, this model will be capable of reproducing structures of various scales, including folds, which are largely preserved in fossil continental crust and represent major structures developed during dominant geodynamic processes such as rifting.

The manuscript was greatly improved by the detailed comments of two anonymous reviewers DC and LL warmly thank the Conseil Régional de Basse-Normandie and the FEDER for the two-years financial of the Chair of Excellence of LL at CRISMAT. MZ thanks Geoprob Project PRIN2012 for financing.

References

- AZPIROZ, M. D. & LLOYD, G. E. 2010. The influence of plagioclase LPO on P-wave anisotropy and seismic reflectivity of metabasites from the lower continental crust. *Geogaceta*, **48**, 199–202.
- BABUSKA, V. & CARA, M. 1991. *Seismic Anisotropy in the Earth*. Springer, Dordrecht, The Netherlands, **10**.
- BAKER, D. R., MANCINI, L., POLACCI, M. & HIGGINS, M. D. 2012. An introduction to the application of X-ray microtomography to the three-dimensional study of igneous rocks. *Lithos*, **148**, 262–276.
- BARBERINI, V., BURLINI, L. & ZAPPONE, A. 2007. Elastic properties, fabric and seismic anisotropy of amphibolites and their contribution to the lower crust reflectivity. *Tectonophysics*, **445**, 227–244.
- BARBOZA, S. A. & BERGANTZ, G. W. 2000. Metamorphism and anatexis in the mafic complex contact aureole, Ivrea Zone, Northern Italy. *Journal of Petrology*, **41**, 1307–1327.
- BARREIRO, J. G. & CATALÁN, J. R. M. 2012. The Bazar shear zone (NW Spain): microstructural and time-of-flight neutron diffraction analysis. In: ZUCALI, M., SPALLA, M. I. & GOSSO, G. (eds) Multiscale structures and tectonic trajectories in active margins. *Journal of the Virtual Explorer*, **41**, Paper 5, <http://dx.doi.org/10.3809/jvirtex.2011.00296>
- BERTOTTI, G., SILETTO, G. B. & SPALLA, M. I. 1993. Deformation and metamorphism associated with crustal rifting: the Permian to Liassic evolution of the Lake Lugano-Lake Como area (Southern Alps). In: CLOETINGH, S., SASSI, W. & HORVATH, F. (eds) *The Origin of Sedimentary Basins: Inferences from Quantitative Modelling and Basin Analysis*. Elsevier, Amsterdam, Netherlands, 271–284.
- BIGI, G., CASTELLARIN, A., COLI, M., DAL PIAZ, G. V., SARTORI, R., SCANDONE, P. & VAI, G. B. 1990. Structural Model of Italy, sheets 1–2: CNR, Progetto Finalizzato Geodinamica.
- BIRCH, F. 1960. The velocity of compressional waves in rocks to 10 kilobars, part 1. *Journal of Geophysical Research*, **65**, 1083–1102.
- BIRCH, F. 1961. The velocity of compressional waves in rocks to 10 kilobars: 2. *Journal of Geophysical Research*, **66**, 2199–2224.
- BLAICH, O. A., FALEIDE, J. I. & TSICALAS, F. 2011. Crustal breakup and continent-ocean transition at South Atlantic conjugate margins. *Journal of Geophysical Research*, **116**, B01402.
- BORIANI, A. & BURLINI, L. 1995. Carta geologica della Valle Cannobina.: Dipartimento di scienze della terra dell'Università degli studi di Milano. Tav. 1.
- BORIANI, A., BURLINI, L. & SACCHI, R. 1990a. The Cossato-Mergozzo-Brissago Line and the Pogallo Line (Southern Alps, Northern Italy) and their relationships with the late-Hercynian magmatic and metamorphic events. *Tectonophysics*, **140**, 193–212.
- BORIANI, A., ORIGONI, E. G., BORGHI, A. & CAIRONI, V. 1990b. The evolution of the 'Serie dei Laghi' (Strona-Ceneri and Scisti dei Laghi): the upper component of the Ivrea-Verbano crustal section; Southern Alps, North Italy and Ticino, Switzerland. *Tectonophysics*, **182**, 103–118.
- BORIANI, A., BURLINI, L. & SACCHI, R. 1990c. The Cossato-Mergozzo-Brissago line and the Pogallo line (Southern Alps, Northern Italy) and their relationships with late-Hercynian magmatic and metamorphic events. *Tectonophysics*, **140**, 193–212.
- BURLINI, L. 1994. A model for the calculation of the seismic properties of geologic units. *Surveys in Geophysics*, **15**, 593–617.
- BURLINI, L. & FOUNTAIN, D. M. 1993. Seismic anisotropy of metapelites from the Ivrea-Verbano zone and Serie dei Laghi (northern Italy). *Physics of the Earth and Planetary Interiors*, **78**, 301–317.
- CASTELLANZA, R., GEROLYMATOU, E. & NOVA, R. 2008. An attempt to predict the failure time of abandoned mine pillars. *Rock Mechanics and Rock Engineering*, **41**, 377–401.
- CHRISTENSEN, N. I. 1984. The magnitude, symmetry and origin of upper mantle anisotropy based on fabric analyses of ultramafic tectonites. *Geophysical Journal of the Royal Astronomical Society*, **76**, 89–111.
- CHRISTENSEN, N. I. & MOONEY, W. D. 1995. Seismic velocity structure and composition of the continental crust: a global view. *Journal of Geophysical Research: Solid Earth (1978–2012)*, **100**, 9761–9788.
- CONNOLLY, J. A. D. 2005. Computation of phase equilibria by linear programming: A tool for geodynamic modeling and its application to subduction zone decarbonation. *Earth and Planetary Science Letters*, **236**, 524–541.
- CONNOLLY, J. A. D. & KERRICK, D. M. 2002. Metamorphic controls on seismic velocity of subducted oceanic crust at 100–250 km depth. *Earth and Planetary Science Letters*, **204**, 61–74.
- CONTRUCCI, I., MATIAS, L. ET AL. 2004. Deep structure of the West African continental margin (Congo,

- Zaire, Angola), between 5 S and 8 S, from reflection/refraction seismics and gravity data. *Geophysical Journal International*, **158**, 529–553.
- DALE, J., HOLLAND, T. & POWELL, R. 2000. Hornblende-garnet-plagioclase thermobarometry: a natural assemblage calibration of the thermodynamics of hornblende. *Contributions to Mineralogy and Petrology*, **140**, 353–362.
- GIOBBI MANCINI, E., BORIANI, A. & VILLA, I. 2003. Pre-Alpine ophiolites in the basement of southern Alps; the presence of a bimodal association (LAG-Leptyno-Amphibolitic Group) in the Serie dei Laghi (N-Italy, Ticino-CH). *Rendiconti Fisica Accademia dei Lincei*, **9**, 79–99.
- HANDY, M. R. 1987. The structure, age and kinematics of the Pogallo fault zone; southern Alps, north-western Italy. *Eclogae Geologicae Helveticae*, **80**, 593–632.
- HANDY, M. R., FRANZ, L., HELLER, F., JANOTT, B. & ZURBRIGGEN, R. 1999. Multistage accretion and exhumation of the continental crust (Ivrea crust section, Italy and Switzerland). *Tectonics*, **18**, 1154–1177.
- HANDY, M. R., SCHMID, S., BOUSQUET, R., KISSLING, E. & BERNOULLI, D. 2010. Reconciling plate-tectonic reconstructions of Alpine Tethys with the geological–geophysical record of spreading and subduction in the Alps. *Earth-Science Reviews*, **102**, 121–158.
- HENK, A., FRANZ, L., TEUFEL, S. & ONCKEN, O. 1997. Magmatic underplating, extension, and crustal reequilibration: insights from a cross section through the Ivrea zone and Strona–Ceneri zone, Northern Italy. *Journal of Geology*, **105**, 367–377.
- HILL, R. 1952. The elastic behaviour of a crystalline aggregate. *Proceedings of the Physical Society of London*, **65**, 351–354.
- HIRSCH, K. K., BAUER, K. & SCHECK-WENDEROTH, M. 2009. Deep structure of the western South African passive margin – results of a combined approach of seismic, gravity and isostatic investigations. *Tectonophysics*, **470**, 57–70.
- HOLLAND, T. J. B. & POWELL, R. 1998. An internally consistent thermodynamic data set for phases of petrological interest. *Journal of Metamorphic Geology*, **16**, 309–344.
- ISMAÏL, W. B. & MAINPRICE, D. 1998. An olivine fabric database: an overview of upper mantle fabrics and seismic anisotropy. *Tectonophysics*, **296**, 145–157.
- Ji, S. & LONG, C. 2006. Seismic reflection response of folded structures and implications for the interpretation of deep seismic reflection profiles. *Journal of Structural Geology*, **28**, 1380–1387.
- Ji, S. & MAINPRICE, D. 1990. Recrystallization and fabric development in plagioclase. *Journal of Geology*, **98**, 65–79.
- Ji, S. & XIA, B. 2002. *Rheology of Polyphase Earth Materials*. Polytechnic International Press, Canada, 260 pp.
- KARATO, S. 2008. *Deformation of Earth Materials: An Introduction to the Rheology of Solid Earth*. Cambridge University Press, Cambridge.
- KERN, H., BURLINI, L. & ASHCHEPKOV, I. V. 1996. Fabric-related seismic anisotropy in upper-mantle xenoliths: evidence from measurements and calculations. *Physics of the Earth and Planetary Interiors*, **95**, 195–209.
- KERN, H., MENGEL, K., STRAUSS, K. W., IVANKINA, T. I., NIKITIN, A. N. & KUKKONEN, I. T. 2009. Elastic wave velocities, chemistry and modal mineralogy of crustal rocks sampled by the Outokumpu scientific drill hole: evidence from lab measurements and modeling. *Physics of the Earth and Planetary Interiors*, **175**, 151–166.
- KHAZANEHDARI, J., RUTTER, E. H. & BRODIE, K. H. 2000. High-pressure-high-temperature seismic velocity structure of the midcrustal and lower crustal rocks of the Ivrea-Verbano zone and Serie dei Laghi, NW Italy. *Journal of Geophysical Research*, **105**, 13.
- KITAMURA, K. 2006. Constraint of lattice-preferred orientation (LPO) on Vp anisotropy of amphibole-rich rocks. *Geophysical Journal International*, **165**, 1058–1065.
- LENTINI, M. R., FRASER, S. I., SUMNER, H. S. & DAVIES, R. J. 2010. Geodynamics of the central South Atlantic conjugate margins: implications for hydrocarbon potential. *Petroleum Geoscience*, **16**, 217–229.
- LIANG, L., RINALDI, R. & SCHÖBER, H. 2008. *Neutron Applications in Earth, Energy and Environmental Sciences*. Springer-Verlag, New York, USA.
- LLOYD, G. E., BUTLER, R. W. H., CASEY, M., TATHAM, D. J. & MAINPRICE, D. 2011a. Constraints on the seismic properties of the middle and lower continental crust. PRIOR, D. J., RUTTER, E. H. & TATHAM, D. J. (eds) *Deformation Mechanisms, Rheology and Tectonics: Microstructures, Mechanics and Anisotropy*. Geological Society, London, Special Publications, **360**, 7–32.
- LLOYD, G. E., HALLIDAY, J. M., BUTLER, R. W. H., CASEY, M., KENDALL, J.-M., WOOKEY, J. & MAINPRICE, D. 2011b. From crystal to crustal: petrofabric-derived seismic modelling of regional tectonics. In: PRIOR, D. J., RUTTER, E. H. & TATHAM, D. J. (eds) *Deformation Mechanisms, Rheology and Tectonics: Microstructures, Mechanics and Anisotropy*. Geological Society, London, Special Publications, **360**, 49–78.
- LUTTEROTTI, L., MATTHIES, S. & WENK, H. R. 1999. MAUD (Material Analysis Using Diffraction): a user friendly Java program for Rietveld Texture Analysis and more. *Proceedings of the Twelfth International Conference on Textures of Materials (ICOTOM-12)*, **2**, 1599.
- LUVIZOTTO, G. L. & ZACK, T. 2009. Nb and Zr behavior in rutile during high-grade metamorphism and retrogression: an example from the Ivrea–Verbano Zone. *Chemical Geology*, **261**, 303–317.
- MAINPRICE, D. 1990. A FORTRAN program to calculate seismic anisotropy from the lattice preferred orientation of minerals. *Computers & Geosciences*, **16**, 385–393.
- MAINPRICE, D. & NICOLAS, A. 1989. Development of shape and lattice preferred orientations: Application to the seismic anisotropy of the lower crust. *Journal of Structural Geology*, **11**, 391–398.
- MAINPRICE, D., SILVER, P. G. & NICOLAS, A. 1993. Seismic anisotropy in the mantle from petrofabric. *Eos Transactions of American Geophysical Union*, **74**, 203.
- MAINPRICE, D., HIELSCHER, R. & SCHAEUBEN, H. 2011. Calculating anisotropic physical properties from texture data using the MTEX open-source package.

3D MICROSTRUCTURAL ANALYSIS OF SOUTHERN ALPS AMPHIBOLITE

- In: PRIOR, D. J., RUTTER, E. H. & TATHAM, D. J. (eds) *Deformation Mechanisms, Rheology and Tectonics: Microstructures, Mechanics and Anisotropy*. Geological Society, London, Special Publications, **360**, 175–192.
- MATTHIES, S. & VINEL, G. W. 1982. On the reproduction of the orientation distribution function of textured samples from reduced pole figures using the concept of ghost correction. *Physica Status Solidi (a)*, **112**, K111–K114.
- MAZZUCHELLI, M., ZANETTI, A., RIVALENTI, G., VANNUCCI, R., CORREIA, C. T. & TASSINARI, C. C. G. 2010. Age and geochemistry of mantle peridotites and diorite dykes from the Baldissero body: insights into the Paleozoic–Mesozoic evolution of the Southern Alps. *Lithos*, **119**, 485–500.
- MEISSNER, R., RABEL, W. & KERN, H. 2006. Seismic lamination and anisotropy of the lower continental crust. *Tectonophysics*, **416**, 81–99.
- MUTTONI, G., KENT, D. V., GARZANTI, E., BRACK, P., ABRAHAMSEN, N. & GAETANI, M. 2003. Early Permian Pangea ‘B’ to Late Permian Pangea ‘A’. *Earth and Planetary Science Letters*, **215**, 379–394.
- NEWTON, R. C., CHARLU, T. V. & KLEPPA, O. J. 1980. Thermochemistry of the high structural state plagioclases. *Geochimica et Cosmochimica Acta*, **44**, 933–941.
- OUTLAW, R. K., ERICKSON, R. C. & DEIBERT, J. 2000. Petrology of a meta-anorthositic gabbro block, Franciscan Complex, Sonoma County, California Geological Society of America. In: WEIGAND, P. W. & SHELLBARGER, J. (eds) *Cordilleran Section, 97th Annual Meeting; AAPG Pacific Section, Annual Meeting*. Geological Society of America (GSA), Boulder, CO, United States.
- PASSCHIER, C. W. & TROUW, R. A. J., 2005. *Microtectonics*. Springer, Germany.
- PERESSINI, G., QUICK, J. E., SINIGOI, S., HOFMANN, A. W. & FANNING, M. 2007. Duration of a large mafic intrusion and heat transfer in the lower crust: a SHRIMP U–Pb zircon study in the Ivrea–Verbano Zone (Western Alps, Italy). *Journal of Petrology*, **48**, 1185.
- QUICK, J. E., SINIGOI, S. & MAYER, A. 1994. Emplacement dynamics of a large mafic intrusion in the lower crust, Ivrea–Verbano Zone, Northern Italy. *Journal of Geophysical Research*, **99**, 21 559–21 573.
- QUICK, J. E., SINIGOI, S. & MAYER, A. 1995. Emplacement of mantle peridotite in the lower continental crust, Ivrea–Verbano zone, northwest Italy. *Geology*, **23**, 739–742.
- RABEL, W. & MOONEY, W. D. 1996. Seismic anisotropy of the crystalline crust: what does it tell us? *Terra Nova*, **8**, 16–21.
- RIVALENTI, G., GARUTI, G., ROSSI, A., SIENA, F. & SINIGOI, S. 1981. Existence of different peridotite types and of a layered igneous complex in the Ivrea zone of the Western Alps. *Journal of Petrology*, **22**, 127–153.
- RUDNICK, R. L. & FOUNTAIN, D. M. 1995. Nature and composition of the continental crust: a lower crustal perspective. *Reviews of Geophysics*, **33**, 267–309.
- RUDNICK, R. L. & GAO, S. 2003. Composition of the continental crust. *Treatise on Geochemistry*, **3**, 1–64.
- RUTTER, E., KHAZANEHDARI, J., BRODIE, K. H., BLUNDELL, D. J. & WALTHAM, D. A. 1999. Synthetic seismic reflection profile through the Ivrea Zone–Serie dei Laghi continental crustal section, northwestern Italy. *Geology (Boulder)*, **27**, 79–82.
- RUTTER, E., BRODIE, K., JAMES, T. & BURLINI, L. 2007. Large-scale folding in the upper part of the Ivrea–Verbano zone, NW Italy. *Journal of Structural Geology*, **29**, 1–17.
- SAKATA, M., UNO, T., TAKATA, M. & HOWARD, C. J. 1993. Maximum-entropy-method analysis of neutron diffraction data. *Journal of Applied Crystallography*, **26**, 159–165.
- SHIGEMATSU, N. & TANAKA, H. 1999. Dislocation creep of fine-grained recrystallized plagioclase under low-temperature conditions. *Journal of Structural Geology*, **22**, 65–79.
- SIEGSMUND, S., TAKESHITA, T. & KERN, H. 1989. Anisotropy of V_p and V_s in an amphibolite of the deeper crust and its relationship to the mineralogical, microstructural and textural characteristics of the rock. *Tectonophysics*, **157**, 25–38.
- SPALLA, M. I. & MAROTTA, A. M. 2007. P–T evolutions v. numerical modelling: a key to unravel the Paleozoic to early-Mesozoic tectonic evolution of the Alpine area. *Periodico di Mineralogia*, **76**, 267–308.
- SPALLA, M. I., SILETTO, G. B., DI PAOLA, S. & GOSSO, G. 2000. The role of structural and metamorphic memory in the distinction of tectono-metamorphic units: the basement of the Como lake in the Southern Alps. *Journal of Geodynamics*, **30**, 191–204.
- SPALLA, M. I., ZUCALI, M., DI PAOLA, S. & GOSSO, G. 2005. A critical assessment of the tectono-thermal memory of rocks and definition of the tectonometamorphic units: evidence from fabric and degree of metamorphic transformations. In: GAPAIS, D., BRUN, J. P. & COBBOLD, P. (eds) *Deformation Mechanisms, Rheology and Tectonics: from Minerals to the Lithosphere*. Geological Society, London, Special Publications, **243**, 227–247.
- SPALLA, M. I., GOSSO, G., MAROTTA, A. M., ZUCALI, M. & SALVI, F. 2010. Analysis of natural tectonic systems coupled with numerical modelling of the polycyclic continental lithosphere of the Alps. *International Geology Review*, **52**, 1268–1302.
- STAMPFLI, G. M. & BOREL, G. D. 2002. A plate tectonic model for the Paleozoic and Mesozoic constrained by dynamic plate boundaries and restored synthetic oceanic isochrons. *Earth and Planetary Science Letters*, **196**, 17–33.
- TARTAROTTI, P., ZUCALI, M., PANSERI, M., LISSANDRELLI, S., CAPELLI, S. & OULADDIAF, B. 2011. Mantle origin of the Antrona serpentinites (Antrona ophiolite, Pennine Alps) as inferred from microstructural, microchemical, and neutron diffraction quantitative texture analysis. *Ophioliti*, **36**, 167–189.
- TATHAM, D. J., LLOYD, G. E., BUTLER, R. W. H. & CASEY, M. 2008. Amphibole and lower crustal seismic properties. *Earth and Planetary Science Letters*, **267**, 118–128.
- TOMMASI, A., GILBERT, B., SEIPOLD, U. & MAINPRICE, D. 2001. Anisotropy of thermal diffusivity in the upper mantle. *Nature*, **411**, 783–786.

- TURNER, F. J. & WEISS, L. E. 1963. *Structural Analysis of Metamorphic Tectonites*. MacGraw-Hill, New York.
- VAVRA, G., SCHMID, R. & GEBAUER, D. 1999. Internal morphology, habit and U–Th–Pb microanalysis of amphibolite-to-granulite facies zircons: geochronology of the Ivrea Zone (Southern Alps). *Contributions to Mineralogy and Petrology*, **134**, 380–404.
- VOLTOLINI, M., ZANDOMENEGHI, D., MANCINI, L. & POLACCI, M. 2011. Texture analysis of volcanic rock samples: quantitative study of crystals and vesicles shape preferred orientation from X-ray microtomography data. *Journal of Volcanology and Geothermal Research*, **202**, 83–95.
- WENK, H. R. 2006. Neutron diffraction texture analysis. In: WENK, R. (ed.) *Neutron Scattering in Earth Sciences, Reviews in Mineralogy and Geochemistry*. Mineralogical Society of America, USA, **63**, 399–426.
- WENK, H. R., MATTHIES, S., DONOVAN, J. & CHATEIGNER, D. 1998. Beartex: a Windows-based program system for quantitative texture analysis. *Journal of Applied Crystallography*, **31**, 262–269.
- WHITE, R. W., POWELL, R. & HOLLAND, T. J. B. 2001. Calculation of partial melting equilibria in the system Na₂O–CaO–K₂O–FeO–MgO–Al₂O₃–SiO₂–H₂O (NCKFMASH). *Journal of Metamorphic Geology*, **19**, 139–153.
- WOLFF, R., DUNKL, I., KIESSELBACH, G., WEMMER, K. & SIEGESMUND, S. 2012. Thermochronological constraints on the multiphase exhumation history of the Ivrea-Verbano Zone of the Southern Alps. *Tectonophysics*, **579**, 104–117.
- ZINGG, A. 1983. The Ivrea and Strona Ceneri zones (Southern Alps, Ticino and Northern Italy): a review. *Schweizerische Mineralogische petrographische Mitteilungen*, **63**, 361–392.
- ZUCALI, M., CHATEIGNER, D., DUGNANI, M., LUTTEROTTI, L. & OULADDIAF, B. 2002. Quantitative texture analysis of naturally deformed hornblendite under eclogite facies conditions (Sesia-Lanzo Zone, Western Alps): comparison between x-ray and neutron diffraction analysis. In: DE MEER, S., DRURY, M. R., DE BRESSER, J. H. P. & PENNOCK, G. M. (eds) *Deformation Mechanisms, Rheology and Tectonics: Current Status and Future Perspectives*. Geological Society, London, Special Publications, **200**, 239–253.
- ZUCALI, M., BARBERINI, V., CHATEIGNER, D., OULADDIAF, B. & LUTTEROTTI, L. 2010. Brittle plus plastic deformation of gypsum aggregates experimentally deformed in torsion to high strains: quantitative microstructural and texture analysis from optical and diffraction data. In: SPALLA, M. I., MAROTTA, A. M. & GOSSO, G. (eds) *Advances in Interpretation of Geological Processes: Refinement of Multi-scale Data and Integration in Numerical Modelling*. Geological Society, London, Special Publications, **332**, 79–98.
- ZUCALI, M., TARTAROTTI, P., CAPELLI, S. & OULADDIAF, B. 2012. Multiscalar structural study of the ultramafic rocks of the Antrona ophiolite (Pennine Alps). *Journal of the Virtual Explorer*, **41**, 4.
- ZUCALI, M., VOLTOLINI, M., OULADDIAF, B., MANCINI, L. & CHATEIGNER, D. 2014. The 3D quantitative lattice and shape preferred orientation of a mylonitised metagranite from Monte Rosa (Western Alps): combining neutron diffraction texture analysis and synchrotron X-ray microtomography. *Journal of Structural Geology*, **63**, 91–105, <http://dx.doi.org/10.1016/j.jsg.2014.02.011>